CHEMISTRY
A EUROPEAN JOURNAL

DOI: 10.1002/chem.200700943

Ion-Conduction Pathways in Self-Organised Ureidoarene–Heteropolysiloxane Hybrid Membranes

Mathieu Michau,[a] Mihail Barboiu,*[a] Rémi Caraballo,[a] Carole Arnal-Hérault,[a] Pascal Perriat,[b] Arie van der Lee,[a] and A. Pasc[a]

Abstract: This paper reports on hybrid organic–inorganic dense membrane materials in which protons and ions are envisioned to diffuse along the hydrophilic pathways. The hierarchical generation of functional hybrid materials was realised in two steps. First, the self-assembling properties of 3-(ureidoarene)propyltriethoxysilane compounds **1**–**5** in aprotic solvents were determined, revealing the formation of supramolecular oligomers. Compounds **1**–**5** generate organogels in chloroform or in acetone, leading in a second sol–gel transcription step to hybrid membrane materials on a nanoscopic scale. The crystal structures of **1**–**5** indicate that the arrangement is mainly defined by periodic parallel sheets, resulting from the alignment of hydrophobic organic and inorganic silica layers. Hybrid materials **MB1**–**MB4**, with a similar lamellar structure, define particularly attractive functional transport devices; they are oriented along the organic layers and sandwiched between the two siloxane layers. These systems have been employed successfully to design solid dense membranes and illustrate how the self-organised hybrid materials perform interesting and potentially useful functions.

Keywords: membranes · molecular devices · organic–inorganic hybrid composites · self-assembly · sol–gel processes

Introduction

Many fundamental biological processes appear to depend on the unique properties of the hydrophilic domains of biomolecules. Such behaviour is illustrated by the functional complexity of self-organised membrane proteins, which may assist in proton and ion translocation through membranes.[1] Gramicidin A,[2] the KCsA K^+ channel,[3] and Aquaporin water channels[4] are well-known non-exclusive examples of functional systems in which protons, ions and water molecules are envisioned to diffuse along a directional pathway according to different relaying and migration mechanisms.[1–6]

Numerous artificial transport systems utilizing carriers, channel-forming or self-organised polymeric superstructures able to orient, select, and pump the ionic transport across membranes, have been developed in the last few decades. Crown ethers,[7] cyclic peptides,[8] oligophenyl barrel–stave structures[9] and oligoester bolaamphiphiles[10] have all been used in this context, mostly in lipid bilayers. Functional crystalline organic[11] or inorganic materials,[12] polymeric[13] or dendrimeric[14] self-organised devices, designed to mimic natural ion channel proteins, moved the field of bio-inspired supramolecular frameworks to a nanometric scale.

Hybrid organic–inorganic materials produced by sol–gel processes are the subject of various investigations, offering the opportunity to achieve nanostructured functional materials.[15] These materials reveal great potential on the level of their chemical composition or organisation and in terms of the applications concerned.[15a–c] Organogels resulting from multiple self-assembly processes and acting as robust organic templates for the TEOS sol–gel process (TEOS = tetraethoxysilane) have been used for the synthesis of different inorganic structures.[15d] Many groups, including our own, have found new methods for the elaboration of hybrid self-organised materials based on silsesquioxanes, in which the

---

[a] Dr. M. Michau, Dr. M. Barboiu, R. Caraballo, Dr. C. Arnal-Hérault,
Dr. A. van der Lee, Dr. A. Pasc
Adaptative Supramolecular Nanosystems Group
Institut Européen des Membranes
ENSCM/UMII/UMR-CNRS 5635, Place Eugène Bataillon
CC 47, 34095 Montpellier, Cedex 5 (France)
Fax: (+33) 467-14-91-19
E-mail: barboiu@iemm.univ-montp2.fr

[b] Dr. P. Perriat
MATEIS (GEMPPM) UMR-CNRS 5510, INSA de Lyon
Batiment, Blaise Pascal
7 Avenue Jean capelle, 69621 Villeurbane, Cedex (France)

Supporting information for this article is available on the WWW under http://www.chemeurj.org/ or from the author.

functional organic (supramolecular) and inorganic siloxane networks are covalently connected. Rigid aromatic molecules[15e–g] and urea ribbons[15h–k,16] are used to transcribe an oriented supramolecular self-organisation in a siloxane matrix by a sol–gel process. Of particular interest is the structure-directed function of hybrid materials and the control of their build-up by self-organisation. Recently, we proved the possibility of creating hybrid macrocyclic complexant membranes, self-organised in directional tubular superstructures. They have been employed successfully to design an ion-powered ATP^{2-} pump.[16]

However, the structural functionality of membrane proteins is not defined by the specific complexant receptors. Very simple functional moieties (i.e., carbonyl, hydroxyl, amide, etc.) point towards the protein core that surrounds the transport direction. The end result when such moieties come together is a supramolecular organisation of binding sites collectively contributing to the selective translocation of solutes along the protein wall.[2–4] Toward this objective, our aim is to develop new functional hybrid membrane materials by using simple molecules bearing hydrophilic moieties that form patterns by collective self-assembly so as to enable efficient translocation events. Herein we describe several findings related to this aim, and we report new hybrid organic–inorganic dense materials in which protons and ions are envisioned to diffuse along *hydrophilic pathways*. The hierarchical generation of functional hybrid materials was realised in two steps. First, the self-assembling properties of 3-(ureidoarene)propyltriethoxysilane compounds **1**–**5** in aprotic solvents were determined, revealing the formation of supramolecular oligomers. They generate organogels in chloroform or acetone, leading in a second *sol–gel transcription* step to hybrid membrane materials on a nanoscopic scale. Finally they were tested in dialysis transport experiments.

Results and Discussion

Synthesis of alkoxysilane precursors 1–5 and self-organised hybrid materials MB 1–MB 4, MB 1*–MB 4*: Five 3-(ureidoarene)propyltriethoxysilane compounds (**1**–**5**) were prepared for the studies described here (Scheme 1). We restricted our studies to benzene-, indole-, and phenol-derivatives **1**–**3**, respectively, which are the arene (Ar) termini of phenylalanine, tryptophan, and tyrosine, respectively, three aromatic essential amino acids. The methoxybenzene **4** and hydroxymethylbenzene **5** moieties were chosen for the structural studies described later. The 3-isocyanatopropyltriethoxysilane was treated with the corresponding aromatic amine ($CHCl_3$, 80 °C, 5 h) to afford after crystallisation **1**–**5** as white powders.

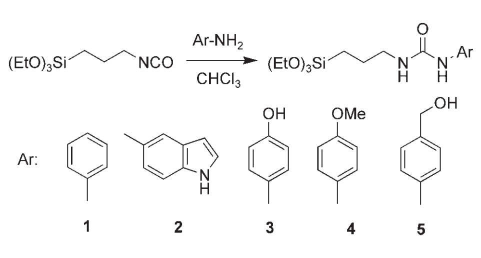

Scheme 1.

The generation of self-organised superstructures in solution, sols, gels, and in the solid state, is based on three encoded features:

1) They contain an hydrophilic arene moiety (except **1**); the importance of interactions between alkali cations and side chains of aromatic amino acids has been known for many years and they are of particular biological significance;[3,5,7a]
2) The supramolecular guiding interaction is the urea head-to-tail hydrogen-bond association,[9a] similar to the hydrogen bonding of the amide moieties in proteins
3) These ureido–aromatic residues are covalently bonded to triethoxysilyl groups, allowing them, by a sol–gel process, to transcribe their self-organised superstructures formed in solutions and gels to the hybrid materials.

^1H NMR spectra of solutions of **1**–**5** show a strong downfield shift of both NH protons upon increasing the concentration in $CDCl_3$, which is indicative of self-association through intermolecular hydrogen bonding.[18] The association of species **1**–**5** diminishes from $\mathbf{1}\cong\mathbf{5}>\mathbf{4}>\mathbf{2}>\mathbf{3}$ (Figure 1). The most associated compounds (**1**, **4** and **5**) contain a hydrophobic sidearm. The formation of aggregates is probably hindered when supplementary hydrogen-bonding residues (**2** and **3**) are present.

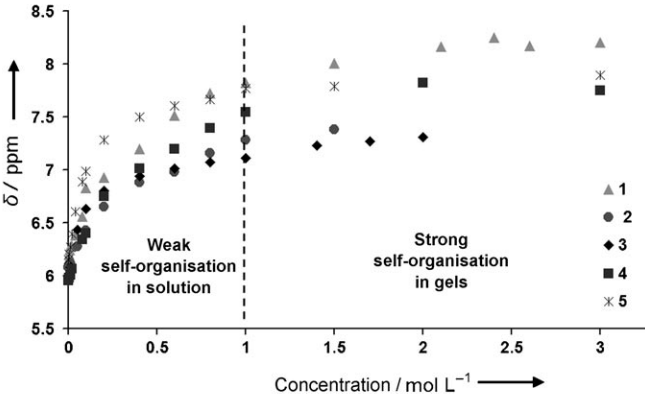

Figure 1. Chemical shifts of the N−H_1 protons plotted against the concentration of **1**–**5** at 25 °C.

Compounds **1**–**5** can gelate the solvents acetone and chloroform ($C>1$, Figure 1). To limit the cross-linking of the siloxane network favoured by hydrolysis, and to maximise the self-organisation of molecular organic moieties, we conducted the sol–gel experiments using mild hydrolysis–condensation conditions:

1) The first strategy was to use heterogeneous acidic catalysis in aprotic solvents, as previously reported by us[16c] and by others.[15k]
2) The second method makes use of diphenyldichlorosilane (Ph_2SiCl_2) as the organic initiator after reaction with the residual water in the reaction medium.

The membranes **MB1**–**MB4** (acidic catalysis) and **MB1***–**MB4*** (organic catalysis) were obtained by coating the sol onto planar polyvinylidenedifluoride (PVDF) supports by using a tape-casting method. By using similar experimental conditions, the **MB5** hybrid material precipitates after the sol-gel process, and therefore only inhomogeneous membrane films were prepared from compound **5**.

FTIR and NMR spectroscopic analyses of precursors **1**–**5** and of solids **MB1**–**MB4** and **MB1***–**MB4*** demonstrate the formation of self-organised hybrid materials. FTIR spectra of the hybrid materials show the appearance of broad vibrations of the $\nu_{\text{Si-O-Si}} = 1000–1200\,\text{cm}^{-1}$ instead of the vibrations $\nu_{\text{Si-OEt}} = 950$, 1070, and $1100\,\text{cm}^{-1}$, initially observed for the molecular precursors **1**–**5**. Evidence for strong urea hydrogen bonding was obtained from the FTIR spectra of solids **MB1**–**MB4** and **MB1***–**MB4***: hydrogen-bond vibration shifts of the urea moiety were detected: $\nu_{\text{N-H}} = 3310$ ($\Delta\nu = 30$), $\nu_{\text{C=O}} = 1630$ ($\Delta\nu = 15$) and $\nu_{\text{C-N}} = 1570\,\text{cm}^{-1}$ ($\Delta\nu = 25$).[17b,c] Moreover we observed a widening of the $\nu_{\text{N-H}} = 3300\,\text{cm}^{-1}$ vibration band, resulting from the superposition of several signals. ^{29}Si MAS NMR spectroscopic experiments are in agreement with the ≈70% condensed hybrid materials **MB1**–**MB4** and **MB1***–**MB4***.

Additional information concerning the self-organisation is obtained from the single-crystal structures and the X-ray powder diffraction analyses of compounds **1**–**5**. Crystals suitable for X-ray structure determination were obtained after a few days in acetone ($c = 0.1\,\text{g mL}^{-1}$) at −10 °C. The molecular structures and packing are presented in Figures 2 and 3. They reveal the expected 3-(ureiodoarene)propyltriethoxysilanes structures of **1**–**5**. Each unit cell contains four molecules, except compound **3** (eight molecules). The urea moiety and the aromatic ring are disposed in an angular position with respect to the arene plane. The H···O distances of 2.04–2.08 Å are the same along the urea ribbon and are consistent with other urea systems.[17] The relative arrangement of the 3-(ureiodoarene)propyltriethoxysilane compounds **1**–**5** in the crystal is similar to previously reported benzocrown-ether-type superstructures.[16d] As shown in Figure 1, the molecules of **1**–**5** are organised in the anti-parallel hydrogen-bonded aggregates. In the crystal lattice the compounds **1**–**5** pack in one direction into ureiodoarene and triethoxysilane layers, each of about 3 Å thickness, which are alternately stratified and present a tight contact (Figure 3). For compounds **2** and **3**, there is a very interesting "communicative" interaction between the organic and inorganic networks, corresponding to hydrogen-bonding contacts between the −NH (**2**) and the −OH (**3**) groups and a neighbouring triethoxysilane moiety ($d_{\text{H···O}} = 1.83$ Å). Moreover the phenolic group is simultaneously hydrogen bonded to the hydroxyl of a neighbouring molecule of **3** ($d_{\text{H···O}} = 1.86$ Å). This results in the internal disruption of the siloxane layers in which these hydrogen-bond interactions occur (Figure 3b,c). Further valuable information was obtained from the crystal structures of the 3-(*p*-methoxybenzeneureido)propyltriethoxysilane (**4**) and the 3-(p-hydroxymethylbenzeneureido)propyltriethoxysilane (**5**) derivatives. The substitution of the −OH group by an −OMe group in compound **4** suppresses the hydrogen-bond communication between the organic and silane networks, leading to a regular directional arrangement of MeO− groups based on hy-

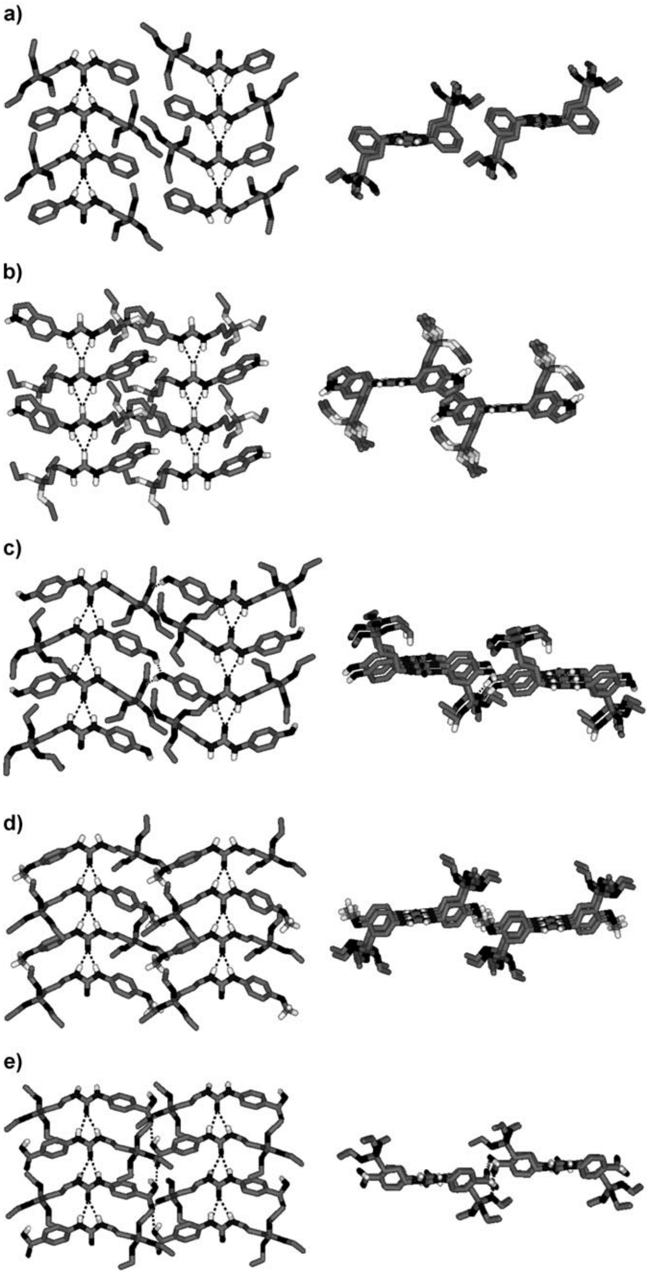

Figure 2. Crystal structures of compounds **1**–**5**: side and top views of the stick representation of H-bonded superstructures of a) **1**, b) **2**, c) **3**, d) **4**, and e) **5**; H atoms are omitted for clarity.

drophobic interactions ($d_{O\cdots O}=5.0$ Å). The −OH group of **5** presents a statistical disorder in the crystal, being simultaneously hydrogen-bonded to the neighbouring $-CH_2OH$ ($d_{O\cdots O}=2.88$ Å) and alkoxysilane groups ($d_{O\cdots O}=2.87$ Å). Accordingly, oriented arrays of hydrogen-bonded $-CH_2OH$ groups, mutually communicating with the inorganic silane layers, are generated in the solid state of **5**. This results in the formation of continual inorganic alkoxysilane layers in the crystal structures of **4** and **5** (Figure 3d,e).

To verify the compatibility of the bulk X-ray fingerprint with the single-crystal structures described before, wet bulk powders of **1**–**5** obtained from evaporation of gels before the sol–gel process were investigated by X-ray powder diffraction. In three cases (**1**, **3** and **5**) a successful identification could be made, which is shown by the Le Bail refinement of the powder patterns in the Supporting Information, Figure 3S a–c. Impurity peaks were found in all cases, representing up to approximately 10% of the weight of the specimen. Since the compounds were found to be chemically pure by NMR spectroscopy, we suppose that either polymorphic forms are present or that slight water uptake and/or polymerisation have taken place. We also note that the crystallinity is not very high in view of the large size of the diffraction peaks. A full Rietveld refinement of the powder diffractograms was attempted with the molecules **1**, **3** and **5** parameterised as rigid bodies. Although the refinements were stable, the Rietveld agreement factors were not very low (≈20%), presumably due to the quality of the diffractograms, which were degraded by the presence of impurity phases and rather large peaks. For compounds **2** and **4** no match could be made between the single-crystal structures and the X-ray powder diffractograms. Therefore the cell parameters of a number of single crystals were tested in order to verify that not an isolated polymorphic variant was picked up to do the full single-crystal structure determination. Since this was not the case, ab initio indexing of the powder patterns was attempted. In the case of **4**, a successful indexing was obtained (M16 = 27.1) with cell parameters $a=15.09$, $b=11.56$, $c=13.09$ Å, $\alpha=90$, $\beta=98.29$ and $\gamma=90°$, for which the volume, $V=2260.7$ Å^3, is interestingly 220 Å^3 larger than the room-temperature volume of the single-crystal structure of **4**; this could correspond to the uptake of three water molecules. For **2** a successful indexation could not be made, which is not surprising in view of its low crystallinity. Compounds **2** and **4** containing indole and methoxyphenyl residues present a second labile interface defined by weak hydrophobic interactions between aromatic units. Simple precipitation of these powders in organic solvents will induce formation of solvated or hydrated polymorphic solids, of different orientations in the solid phase.

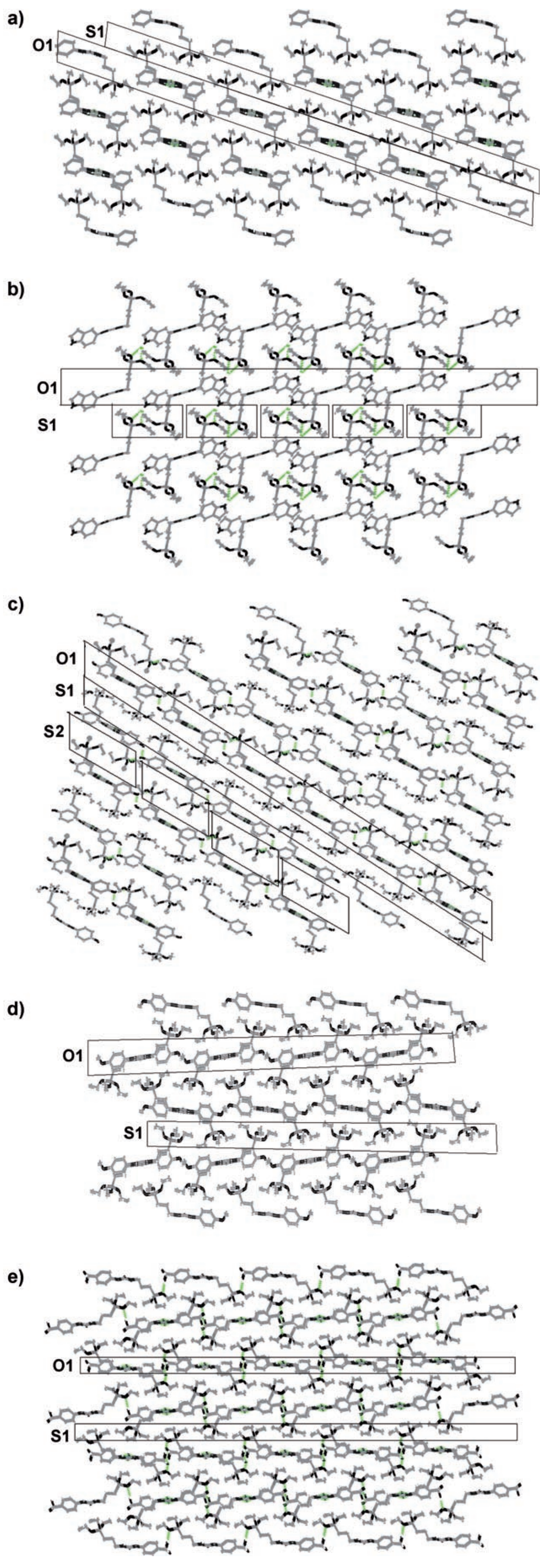

Figure 3. Crystal structures of compounds **1**–**5**: stick representation of crystal packing of a) **1**, b) **2**, c) **3**, d) **4**, and e) **5**; hydrogen-bonds green dotted lines; O1: crystal packing of the organic part; S1, S2: crystal packing of the alkoxysiloxane moieties. The thicknesses of O1, S1 and S2 are about 3 Å.

Unfortunately, the XPRD data show that the hybrid materials **MB 1**–**MB 4** and **MB 1***–**MB 4*** have a different structure compared with their crystalline precursors. The structure change is not surprising, considering that hydrolysis/condensation reactions occur during the sol–gel process.[15,16] For all the hybrids, a successful indexation could not be made, which is not surprising in view of their low crystallinity, confirming the partial loss of order of solvated powders. However, the XRPD patterns of the hybrids show well-resolved peaks, indicating that they are still ordered (Supporting Information, Figure 4 S).

Scanning electron microscopy (SEM) reveals that the thin-layer films (thickness of about 2–3 μm) were dense, without pinholes (Figure 4a). Figure 4b depicts a typical TEM image of an **MB 4** film and shows well-resolved and highly ordered uniform rows with several orientations for the bulk crystalline areas. Since crystallographic symmetry could easily mask a particular TEM distance, it is difficult to compare these distances with those obtained from XPRD patterns of hybrid materials. However, it is clear that the repeating motif is formed by discrete alternative light (inorganic siloxane matrix) and dark (organic self-assembled molecules) rows, with a periodicity in one direction of about 3 Å. The match between these distances and the periodicity of parallel sheets of the self-organised organic and siloxane inorganic networks observed in the crystal packing indicates that the hybrid materials have the same self-organised layered arrangement as observed in the crystal structures (Figure 3).

The X-ray structural data and TEM analysis allow the following conclusions to be drawn:

1) The crystal structures of **1**–**5** indicate that the arrangement is mainly defined by periodic parallel sheets, resulting from the alignment of hydrophobic organic and inorganic silica layers. To our best knowledge, this is the first example of preorganisation of hybrid precursors in which a specific mutual communication between the organic and inorganic networks of hybrid material is defined.
2) A very good compatibility between the wet bulk powders X-ray fingerprint and the single-crystal structure has been found for precursors **1**, **3** and **5**; some deviations from the crystallinity found in the XPRD data of **2** and **4** might either arise from the different orientations of the organic hydrophobic interfaces themselves or from intercalation of solvent or water molecules, defining different polymorphic solids.
3) Hybrid materials **MB 1**–**MB 4** and **MB 1***–**MB 4*** define particularly attractive systems: multioriented nanodomains are well defined (see Figure 4a) starting from molecular components that encode the required informa-

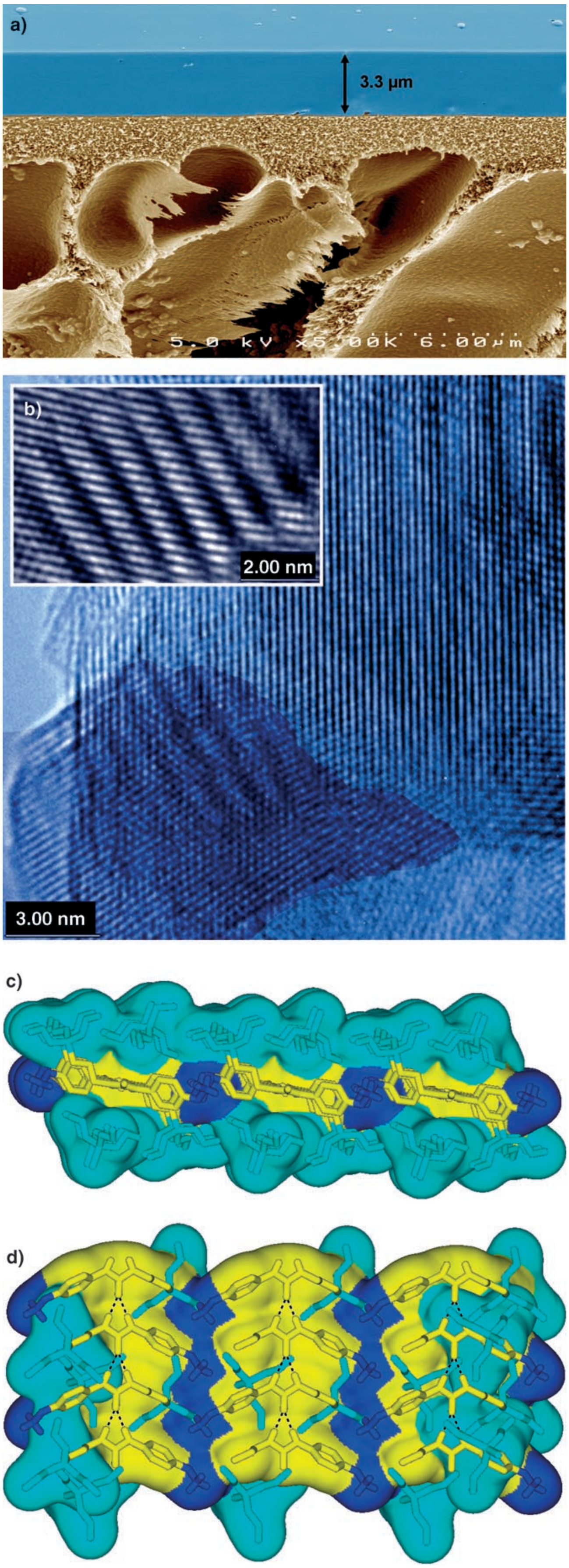

Figure 4. a) SEM image of a hybrid membrane cross-section: the thin-layer dense film deposited onto polymeric PVDF support; b) TEM images of the hybrid material **MB 4**; c) Top view and d) side view of the crystal packing of compound **4** in stick representation with a soft surface.

tion for ionic assisted diffusion within hydrophilic pathways (represented in blue in Figure 4c,d); they are oriented parallel along the hydrophobic organic layers (represented in yellow in Figure 4c,d) and sandwiched between the two hydrophilic siloxane layers (represented in magenta in Figure 4c,d).

Dialysis membrane transport experiments: To demonstrate the generation of *hydrophilic pathways* into hybrid membranes we carried out dialysis transport experiments. (Figure 5).

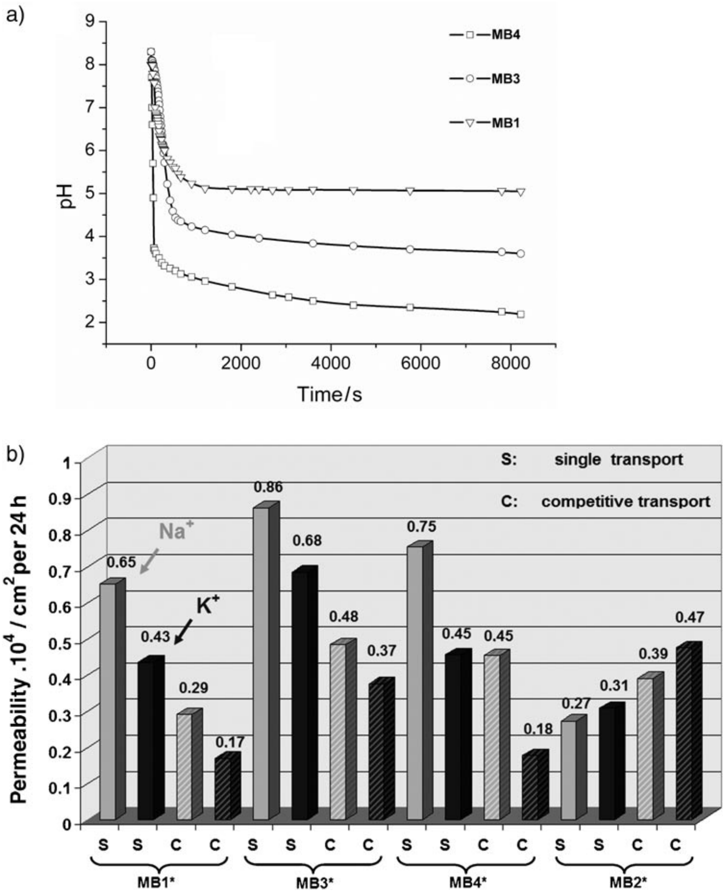

Figure 5. a) pH versus time transport profiles across membranes **MB1**, **MB3**, and **MB4**; b) Permeabilities of **MB1***–**MB4*** hybrid membranes calculated from experimental data using the solution–diffusion model.[20]

The single and competitive H^+, Na^+ and K^+ transport experiments present similar features for both classes of materials **MB1**–**MB4** and **MB1***–**MB4***. In a classical diffusion model the hydrated ions diffuse through the membrane and the mechanism is based on a dual transport mode: solution–diffusion.[20] The transport rate is thus governed by diffusion coefficients and by the interaction equilibria of the hydrated ions losing part of the hydration shell in exchange for the specific complexant groups located in the membrane.

The phenyl-type **MB1** membrane can be considered as a reference membrane in which the transport of ions occurs through a siloxane network containing residual hydrophilic Si–OH groups. The transport of protons (Figure 5a) and alkali cations (Figure 5b) is amplified when phenolic (**MB3**) or methoxyphenyl (**MB4**) groups are present in the membrane. This is consistent with the development of supplementary organic ion-conducting pathways of self-organised –OH and –OMe groups, assisting the diffusion into the hybrid network. The phenolic groups form strong intramolecular hydrogen-bonds with the adjacent –OH, –SiOH and –SiOSi– moieties. This hampers the interactions with surrounding water molecules, and makes the phenolic-type membrane **MB3** more lipophilic than the corresponding methoxyphenyl one **MB4**. Consequently, the protons are better transported along methoxyphenyl pathways within the **MB4** membrane. The dialysis transport experiments were performed by equilibrating the membranes with water. At equilibrium the water uptake might depend on the hydrophilic nature of aromatic group, but the thickness of our active hybrid layers (2–3 μm) do not permit an accurate determination of the amount of water with reference to the supporting membrane. The proton transfer in the membrane occurs by diffusion of $O–H^+ \rightarrow O$ bonds inside the network of hydrophylic pathways, similar to proton transport in water.[2]

The $Na(H_2O)_n^+$ ions are preferentially transported through **MB1**, **MB3** and **MB4** membranes. Since the self-diffusion coefficients $D_{Na(H_2O)_n^+} < D_{K(H_2O)_n^+}$,[21a] the transport of the hydrated cations is probably governed by the solvation free energy, which is thermodynamically more favourable for $Na(H_2O)_n^+$ than $K(H_2O)_n^+$.[21b] Certainly, a substantial contribution to sodium selectivity arises from exchange features between the hydrated ions and hydrophilic moieties located in the membrane. Both hydrated cations are better transported along the more hydrophobic phenolic pathways in the **MB3** membrane. This suggests that they may stay within the hydrophilic methoxy pathways of the **MB4** membrane.

Compared with the reference membrane **MB1** the transport rates of both cations across the indole-type membrane **MB2** decrease. **MB2** is selective for $K(H_2O)_n^+$ ions. Certainly, a substantial contribution to this selectivity arises from exchange features between the hydrated ions and the hydrophobic indole pathways: the complexation of ions by cation–π interactions is thermodynamically more favourable for K^+ ions than Na^+.[21c] Many groups, including our own,[7a,21c,22] have found that the pyrolo subunit of the indole (i.e. $C_2{=}C_3$ bond) is a strong π-donor group for the K^+ ion. This is probably why K^+ ions are preferentially transported within the "indole pathway" of membrane **MB2**.

Conclusion

The controlled formation of such directional transporting devices makes the hybrid membrane materials presented here of interest for the development of a new supramolecular approach to nanoscience through self-organisation, toward hybrid materials of increasing addressability.

The hybrid membrane materials reported in this paper are composed from nanodomains randomly ordered in the hybrid matrix. These oriented nanodomains (Figure 4a) result from the controlled self-assembly of simple molecular components that encode the required information for ionic assisted diffusion within hydrophilic pathways. The novelty of these findings with respect to our previous work[16] with complexant crown ether precursors is that simple molecules, which collectively define transporting devices by self-assembly, can be successfully used to transfer the overall functionality of their supramolecular self-organisation in hybrid membrane materials by sol–gel transcription. Our results imply that the control of molecular interactions can define the self-organised supramolecular architectures presenting a strong communication between the organic and the siloxane layers. We have shown that specific hydrogen-bonding communications between these networks have the ability to create hydrophilic pathways of different chemical properties in the self-organised superstructures of hybrid membrane materials. They are essential in the diffusion process and in the selectivity of the transport of hydrated alkali cations. Although these pathways do not merge to cross the micrometric films, they are well defined along nanometric distances. This is reminiscent of the supramolecular organisation of binding sites in channel-type proteins collectively contributing to the selective translocation of solutes along hydrophilic pathways.[2–4]

Prospects for the future include the development of original methodologies for such communicative transcription in silica matrixes of the supramolecular functional devices, presenting a greater degree of structural complexity.

Experimental Section

Experimental data are available in the Supporting Information. This material includes the general procedure of synthesis and characterisation data (NMR spectroscopy, ESI-MS, elemental analysis) of precursors **1**–**5** and hybrid membrane materials **MB1**–**MB4** and **MB1***–**MB4***. In addition details of X-ray single-crystal diffraction and X-ray powder diffraction, and membrane transport measurements are given.

Acknowledgements

This work, conducted as part of the award “Dynamic adaptive materials for separation and sensing Microsystems” (M.B.) made under the European Heads of Research Councils and European Science Foundation EURYI (European Young Investigator) Awards Scheme in 2004, was supported by funds from the Participating Organisations of EURYI and the EC Sixth Framework Program (see www.esf.org/euryi). This research was supported in part by CNRS and University of Montpellier 2 Montpellier, France.

---

[1] a) F. Hucho, C. Weise, *Angew. Chem.* **2001**, *113*, 3194–3211; *Angew. Chem. Int. Ed.* **2001**, *40*, 3100–3116; b) S. Vaitheeeswaran, H. Yin, J. C. Raisaiah, G. Hummer, *Proc. Natl. Acad. Sci. USA* **2004**, *101*, 17002–17005.

[2] S. Cukierman, *Biophys. J.* **2000**, *78*, 1825–1834.

[3] R. Mackinnon, *Angew. Chem.* **2004**, *116*, 4363–4377; *Angew. Chem. Int. Ed.* **2004**, *43*, 4265–4277.

[4] P. Agre, *Angew. Chem.* **2004**, *116*, 4377–4390; *Angew. Chem. Int. Ed.* **2004**, *43*, 4278–4290.

[5] D. A. Dougherty, *Science* **1996**, *271*, 163–168.

[6] J.P Gallivan, D.A Dougherty, *Proc. Natl. Acad. Sci. USA*, **1999**, *96*, 9459–9464.

[7] a) G. W. Gokel, A. Mukhopadhyay, *Chem. Prod. Chem. Soc Rev.* **2001**, *30*, 274–286; b) N. Voyer, *Top. Curr. Chem.* **1996**, *184*, 1–35.

[8] D. T. Bong, T. D. Clark, J. R. Granja, M. R. Ghadiri, *Angew. Chem.* **2001**, *113*, 1016–1041; *Angew. Chem. Int. Ed.* **2001**, *40*, 988–1011.

[9] a) S. Matile, *Chem. Soc. Rev.* **2001**, *30*, 158–167; b) N. Sakai, J. Mareda, S. Matile, *Acc. Chem. Res.* **2005**, 38, 79–87.

[10] a) P. K. Eggers, T. M. Fyles, ; K. D. D. Mitchell, T. Sutherland, *J. Org. Chem.* **2003**, *68*, 1050–1058; K. D. D. Mitchell, T. Sutherland, *J. Org. Chem.* **2003**, *68*, 1050–1058; b) T. M. Fyles, C. Hu, R. Knoy, *Org. Lett.* **2001**, *3*, 1335–1337.

[11] a) L. E. Cheruzel, M. S. Pometum, M. R. Cecil, M. S. Mashuta, R. J. Wittebort, R. M. Buchanan, *Angew. Chem.* **2003**, *115*, 5610–5613; *Angew. Chem. Int. Ed.* **2003**, *42*, 5452–5455; b) Z. Fei, D. Zhao, T. J. Geldbach, R. Scopelliti, P. J. Dyson, S. Antonijevic, G. Bodenhausen, *Angew. Chem.* **2005**, *117*, 5866–5871; *Angew. Chem. Int. Ed.* **2005**, *44*, 5720–5725.

[12] L. Cronin, *Angew. Chem.* **2006**, *118*, 3656–3658; *Angew. Chem. Int. Ed.* **2006**, *45*, 3576–3578.

[13] *Chem Rev.* **2005**, *105*, Special Issue on Functional Nanostructures.

[14] V. Percec, A. E. Dulcey, M. Peterca, M. Ilies, S. Nurnmelin, M. J. Sienkowska, P. A. Heiney, *Proc. Natl. Acad. Sci. USA* **2006**, *103*, 2518–2523.

[15] a) C. Sanchez, B. Julian, P. Belleville, M. Popall, *J. Mater. Chem.* **2005**, *15*, 3559–3592; b) C. Sanchez, F. Ribot, *New J. Chem.* **1994**, *18*, 1007–1047; c) N. Liu, D. R. Dunphy, M. A. Rodriguez, S. Singer, J. Brinker, *Chem. Commun.*, **2003**, 1144–1145; d) K. J. C. van Bommel, A. Frigerri, S. Shinkai, *Angew. Chem.* **2003**, *115*, 1010–1030; *Angew. Chem. Int. Ed.* **2003**, *42*, 980–999; e) R. J. P. Corriu, *Eur. J. Inorg. Chem.* **2001**, *5*, 1109–1121; f) F. Ben, B. Boury, R. J. P. Corriu, P. Delord, M. Nobili, *Chem. Mater.* **2002**, *14*, 730–738; g) M. P. Kapoor, Q. Yang, S. Inagaki, *J. Am. Chem. Soc.* **2002**, *124*, 15176–11577; h) J. J. E. Moreau, L. Vellutini, M. Wong Chi Man, C. Bied, J. L. Bantignies, P. Dieudonné, J. L. Sauvajol, *J. Am. Chem. Soc.* **2001**, *123*, 7957–7958; i) J. J. E. Moreau, L. Vellutini, M. Wong Chi Man, C. Bied, *Chem. Eur. J.* **2003**, *9*, 1594–1599; j) J. J. E. Moreau, B. P. Pichon, H. Pritzkow, M. Wong Chi Man, C. Bied, J. L. Bantignies, P. Dieudonné, J. L. Sauvajol, *Angew. Chem.* **2004**, *116*, 205–208; *Angew. Chem. Int. Ed.* **2004**, *43*, 203–206; k) O. J. Dautel, J. P. Lère-Porte, J. J. E. Moreau, M. Wong Chi Man, *Chem. Commun.* **2003**, 2662–2663.

[16] a) M. Barboiu, G. Vaughan, A. van der Lee, *Org. Lett.* 2003, 5, 3073–3076; b) M. Barboiu, *J. Inclusion Phenom. Macrocyclic Chem.* **2004**, *49*, 133–137; c) M. Barboiu, S. Cerneaux, A. van der Lee, G. Vaughan, *J. Am. Chem. Soc.* **2004**, *126*, 3545–3550; d) A. Cazacu, C. Tong, A. van der Lee, T. M. Fyles, M. Barboiu, *J. Am. Chem. Soc.* **2006**, *128(29)* 9541–9548; e) C. Arnal-Hérault, A. Banu, M. Barboiu, M. Michau, A. van der Lee, *Angew. Chem.* **2007**, *119*, 4346–4350; *Angew. Chem. Int. Ed.* **2007**, *46*, 4268–4272; f) C. Arnal-Hérault, M. Barboiu, A. Pasc, M. Michau, P. Perriat, A. van der Lee, *Chem. Eur.J* **2007**, *13*, 6792–6800.

[17] a) M. C. Etter, *Acc. Chem. Res.* **1990**, *23*, 120–126; b) J. Van Esch, F. Schoonbeek, M. De Loos, H. Kooijman, A. L. Spek, R. M. Kellog, B. L. Feringa, *Chem. Eur. J.* **1999**, *5*, 937–950; c) F. Schoonbeek, J. Van Esch, B. Wegewijs, D. B. A. Rep, M. P. De Haas, T. M. Klapwijk, R. M. Kellog, B. L. Feringa, *Angew. Chem.* **1999**, *111*, 1486–1490; *Angew. Chem. Int. Ed.* **1999**, *38*, 1393–1397.

[18] Equilibration between hydrogen-bonded and non-hydrogen-bonded states for a given N–H proton is almost always fast on the NMR

timescale, and observed proton chemical shifts are weighted averages of the chemical shifts of contributing states.

[19] The hydrogen-bonding interactions between organic molecules and the silica precursor are determinant for the morphology of the resulted superstructures in the sol–gel transcription processes using heterogeneous organogelator–TEOS systems. See, for instance, J. H. Jung, M. Amaike, S. Shinkai, *Chem. Commun.* **2000**, 2343–2344.

[20] a) M. Barboiu, C. Guizard, C. Luca, B. Albu, N. Hovnanian, J. Palmeri, *J. Membr. Sci.* **1999**, *161*, 193–206; b) M. Barboiu, C. Guizard, N. Hovnanian, J. Palmeri, C. Reibel, C. Luca, L. Cot, *J. Membr. Sci.* **2000**, *172*, 91–103; c) M. Barboiu, C. Guizard, C. Luca, N. Hovnanian, J. Palmeri, L. Cot, *J. Membr. Sci.* **2000**, *174*, 277–286.

[21] Diffusion coefficients in water: $D_{\mathrm{Na^+}} = 1.334\times10^{-9}\,\mathrm{m^2s}$, $D_{\mathrm{K^+}} = 1.957\times10^{-9}\,\mathrm{m^2s}$, a) *Handbook of Chemistry and Physics*, 76th ed., (Ed.: D. R. Lide), **1995/1996**, pp. 5–92; b) C. P. Kelly, C. J. Cramer, D. G. Truhlar, *J. Phys. Chem. B* **2006**, *110*, 16066–16081; c) O. M. Carabacos C. J. Weinheimmer, J. M. Lisy, *J. Chem. Phys.* **1999**, *110*, 8429–8436.

[22] C. Arnal-Herault, M. Barboiu, E. Petit, M. Michau, A. van der Lee, *New J. Chem.* **2005**, *29*, 1535–1539.

Received: June 20, 2007
Revised: October 5, 2007